Follow-on Study on the Applicability of Fly Neighborly Noise Recommendations to UAM Quadrotors in Steady Maneuvers

Sesi Kottapalli*
Aeromechanics Office
NASA Ames Research Center
Moffett Field, CA, USA

D. Douglas Boyd, Jr.
Aeroacoustics Branch
NASA Langley Research Center
Hampton, VA, USA

ABSTRACT

A follow-on study to the 2024 paper by Kottapalli, Silva, and Boyd is presented with improved acoustics tools to examine whether the Vertical Aviation International (VAI) Fly Neighborly operational recommendations that are designed for single main rotor/tail rotor configurations will hold for non-conventional UAM rotorcraft with multiple rotors. The 6-occupant quadrotor concept vehicle designed under the NASA Revolutionary Vertical Lift Technology (RVLT) Project is studied. The tip speed is 550 ft/sec, with three blades per rotor. Predictions are made for three steady maneuvers: level turns, descending turns, and climbing turns. The RVLT Toolchain is exercised using CAMRAD II, pyaaron/AARON/ANOPP2 and AMAT (ANOPP2 Mission Analysis Tool). Quadrotor noise trends are analyzed using Sound Exposure Level (SEL) ground maps because it is anticipated that the upcoming updated Fly Neighborly recommendations will involve SEL maps. Importantly, unlike conventional helicopters with a single main rotor, quadrotor noise can increase in a direction opposite to the turn direction; this finding may need to be taken into consideration in formulating the upcoming updated Fly Neighborly recommendations. The recommendation *Level turns are quieter than descending turns* is followed by this quadrotor under the flight conditions examined. *Turning away from the advancing blade … is quieter than turning into the advancing blade* is not relevant for symmetric aircraft such as the quadrotor. *Straight flight is quieter than turning flight* is not predicted to be best for this quadrotor under the flight conditions examined – turning flight is quieter than straight flight for the quadrotor in this study.

NOTATION

550/3	quadrotor concept vehicle with tip speed=550 ft/sec and 3 blades per rotor
AARON	ANOPP2 Aeroacoustic ROtor Noise tool
AMAT	ANOPP2 Mission Analysis Tool
ANOPP2	Aircraft Noise Prediction Program - Second Generation
BB	broadband noise (trailing-edge self-noise)
BVI	blade vortex interaction
CAMRAD II	Comprehensive Analytical Model of Rotorcraft Aerodynamics and Dynamics II
climb	straight climbing flight
descent	straight descending flight
EPNL	Effective Perceived Noise Level, EPNdB
HAI	Helicopter Association International
left-climb	left turn in climbing flight
left-descent	left turn in descending flight
left-level	left turn in level flight
level	straight level flight
loadz	blade Z-direction (vertical) load in airframe axes, + down, N/m. (-loadz) + up
loadz derivative	derivative of loadz, N/m-deg
OASPL	Overall Sound Pressure Level, dBA
pyaaron	Python tool to aid running AARON
RCOTools	RotorCraft Optimization Tools
RVLT	Revolutionary Vertical Lift Technology Project
right-climb	right turn in climbing flight
right-descent	right turn in descending flight
right-level	right turn in level flight
SEL	Sound Exposure Level, dBA
UAM	Urban Air Mobility
VAI	Vertical Aviation International (formerly HAI)

INTRODUCTION

Recently, Ref. 1 considered the applicability of the Vertical Aviation International (VAI) Fly Neighborly noise recommendations (Ref. 2) to Urban Air Mobility (UAM) quadrotors undergoing steady maneuvers. Figure 1 shows the NASA 6-occupant UAM quadrotor that was considered in Ref. 1. Reference 1 reported on the acoustics of the UAM quadrotor in steady straight flight and steady turning flight (level, climbing and descending, total of nine flight conditions), as summarized in Fig. 2.

This study is a follow-on to Ref. 1 and uses improved and updated acoustics codes. The Fly Neighborly recommendations are currently in the process of being updated. It is anticipated that the new recommendations will involve Sound Exposure Level (SEL) ground noise contour maps. The initial study had considered three ground microphones in a straight line and showed maximum-OASPL and EPNL results. Considering the new upcoming Fly Neighborly recommendations, the current study shows SEL ground noise contours for the same flight conditions as in Ref. 1.

*Corresponding author. Presented at the Vertical Flight Society's 81st Annual Forum & Technology Display, Virginia Beach, VA, USA, May 20-22, 2025.

Previously, Ref. 3 considered the practical conceptual design of quieter urban VTOL aircraft. Several concept vehicles were studied in Ref. 3, including the quadrotor shown in Fig. 1. For this quadrotor, Ref. 4 used the NASA Revolutionary Vertical Lift Technology (RVLT) Toolchain (Ref. 5) to identify and analyze the noise sources. As a follow-on study to Ref. 4 (which had mainly considered rigid blades), Ref. 6 studied the effect of rotor blade elasticity on acoustics for this vehicle.

The tip speed for all rotors is constant at 550 ft/sec, with three blades per rotor (550/3). The blade radius is ~9 ft, and the flight speed is 122 knots. The gross weight is 3,640 lb. Results include vehicle trim and power quantities, vertical blade loading and its azimuthal (or time) derivative, and noise. The blade loading derivative (includes contributions from blade vortex interaction events) is important for the far field loading noise; this is discussed in more detail in a later section.

The Fly Neighborly operational guidelines (Ref. 2) are based on the single main rotor helicopter configuration and are provided in the following section. Several researchers have addressed the acoustics of conventional, single main rotor helicopters undergoing maneuvers (Refs. 7-10). Reference 7 concludes the statement that "A substantial increase in the rotor noise for turning flight was found when compared to level flight at the same speed. This is due to the increased loading a rotor must produce in a turn." Reference 8 presents "the acoustic directivity for a helicopter (both main and tail rotor) in a transient descent condition and compares it to a steady three-degree descent... As a general rule, maneuver tends to increase the intensity of noise and significantly affects its directivity." Also, "The comparison of the two different tail rotors and the main rotor alone demonstrates the importance of including all the rotor noise sources in the acoustic prediction… the various rotors also interact with each other through the balance of forces in the vehicle flight dynamics." (Ref. 8). Reference 9 shows that "Bell 206B Blade Vortex Interaction (BVI) external noise gradually increases in level flight at moderate bank angles and with increasing rates of descent." Based on extensive flight test data, Ref. 10 provides "…validated actionable guidance principles that can be given to pilots to immediately reduce their acoustic footprint during operations. This generic guidance works by keeping the rotor well away from the wake throughout the maneuver, thus increasing miss distance and reducing the occurrence of objectionable BVI noise." For conventional helicopters, Ref. 10 concludes, for example, that noise from level flight turns is not affected by turn direction and level flight turns are quieter than descending turns. Closely related to the conclusions of Ref. 10 are the Fly Neighborly guidelines; these operational recommendations have been published by the Helicopter Association International (HAI, now known as VAI), Ref. 2.

Reference 1 was an initial study on the acoustics of maneuvering non-conventional rotorcraft with multiple rotors (a 6-occupant UAM quadrotor). Reference 1 predicted that the Fly Neighborly guideline that addresses descents (*Level turns are quieter than descending turns*) holds for this UAM quadrotor as well for the flight conditions examined. The current study updates and further analyzes the acoustics of the UAM quadrotor undergoing steady maneuvers. This study examines whether the VAI Fly Neighborly operational recommendations are predicted to hold for this non-conventional rotorcraft with multiple rotors, Fig. 1. The Fly Neighborly guidelines, RVLT Toolchain, and quadrotor modeling are briefly described, followed by the simulation results. The maneuvers considered in this study are steady level turns, steady descending turns, and steady climbing turns. Figure 2 shows the simulation conditions and the flight paths for these turns.

FLY NEIGHBORLY RECOMMENDATIONS

Helicopter noise abatement procedures have been around for decades. As noted earlier, these guidelines are currently being updated. The latest recommendations, published in 2019 (Ref. 2), are listed below. Recommendations relevant to the current study (involving steady maneuvers) are in bold text below.

Level Flight

Accelerations are quieter than decelerations.
Straight flight is quieter than turning flight.

Turning Flight

Turning away from the advancing blade (especially when decelerating) **is quieter than turning into the advancing blade.**
Level turns are quieter than descending turns.

Descending Flight

Straight-in flight is quieter than turning flight.

Decelerations

Level flight decelerations are quieter than descending or turning flight decelerations.

Maneuvering

Smooth and gentle control inputs are quieter than rapid control inputs.

RVLT TOOLCHAIN

The relevant part of the toolchain is discussed in Refs. 4 and 6 and only a summary is provided here. The rotorcraft comprehensive analysis tool CAMRAD II (Comprehensive Analytical Model of Rotorcraft Aerodynamics and Dynamics, Ref. 11) is used to trim the vehicle. RCOTools, a set of Python libraries that serves as application interfaces/wrappers for the execution of CAMRAD II, is also a part of the toolchain (Ref. 12). "pyaaron," a Python-based wrapper script, provides an interface for application-specific user inputs. pyaaron also extracts relevant CAMRAD II data that is then passed on to the acoustic tools.

The acoustic calculations are performed using the following tools:

- AARON (the ANOPP2 Aeroacoustic ROtor Noise tool), Ref. 13. In this context, AARON is an ANOPP2 software tool that runs the ANOPP2 Farassat Formulation 1A Function Model (AF1AIFM) for tonal noise and/or the ANOPP2 Self Noise Internal Function Module (ASNIFM) for rotor broadband self-noise. AARON is used to calculate the 1/3-octave spectrum at each point of a 19x19 hemisphere underneath the vehicle. This calculation is based on the CAMRAD II outputs and a small amount of supplemental information and includes both tone sources (thickness and loading noise) and broadband noise (trailing-edge self-noise), Ref. 1.
- AMAT (ANOPP2 Mission Analysis Tool), Ref. 14. AMAT has been used to predict Noise-Power-Distance data for UAM vehicles (Ref. 15). In the current study, AMAT provides the functionality to model curved flight paths associated with turning flight. For the turning flight cases examined here, the flight path in AMAT is defined using discrete waypoints on a semicircular trajectory (see Fig. 2). For this study, 5 spline-based waypoints were used to define the semicircular trajectory. The 19x19 hemisphere used at each of these waypoints is the same (because all cases are steady state) but oriented at each waypoint such that the front of the hemisphere always points in the direction of flight. For the straight flight path cases examined here, the flight path was defined using two waypoints (start and end points) in AMAT. In all cases, the "top" of the hemisphere is parallel to the flat ground. The vehicle can be banked, pitched, etc. inside the hemisphere. However, the vehicle orientation inside the hemisphere is accounted for by AARON and the vehicle is at the center of the hemisphere.

QUADROTOR MODELING

Quadrotor modeling is the same as that of Ref. 1 except for changes associated with the acoustics tools, such as improvements and updates to the software codes and the run procedures. Figure 1a shows the rotor rotation direction and rotor numbering scheme. The right-front and left-rear rotors (rotors 1 and 4, respectively) turn counterclockwise, and the left-front and right-rear rotors (rotors 2 and 3, respectively) turn clockwise. The CAMRAD II model of the quadrotor is summarized as follows (Refs. 4 and 6): four rotors, rigid uniform blades, collective control, constant RPM, rolled-up free wake (single tip vortex), and longitudinal trim (net zero average vertical and horizontal forces and pitching moment about the aircraft center of gravity). The blades have uniform spanwise inertial and stiffness properties; the blade root includes flap hinge and a pitch bearing. Aerodynamically, the rotors are coupled using wake induced velocities from all rotors. This setting is likely to be the most accurate depiction of the phenomena, capturing potentially important interactions due to strong vortices from not only the other blades on the same rotor, but also from blades of another rotor (rotor-rotor interaction). An important aspect of modeling rotor-rotor interactions is that the vehicle trim is expected to be more accurately modeled. The vehicle trim, including each rotor's thrust, position, and orientation relative to each other and relative to observers, will change the proximity of blade-wake and blade-vortex interactions. Vehicle trim also orients the noise sources, and because of noise directionality, can substantially change the noise magnitude and duration at an observer. Note that the quadrotor in this study was designed with elevated rear rotors to reduce the magnitude of front-rear rotor-rotor interaction; other vehicles may have greater sensitivity to interference in trim and noise results. AARON calculates the 1/3-octave band spectrum at each point of a 19x19 hemisphere (with a radius of 27R and with 10° spacing in both the fore/aft and the lateral directions) underneath the vehicle. The noise calculation is based on the CAMRAD II outputs and a small amount of supplemental information and includes both tonal sources (thickness and loading noise) and broadband noise (trailing edge self-noise), see Ref. 3. AMAT is used to model curved flight paths associated with turning flight.

RESULTS

Noise predictions for straight and steady turning flight (level, climbing and descending, total of nine steady flight conditions, Fig. 2) are presented. The results have been obtained for the 550/3 RVLT concept quadrotor (tip speed is 550 ft/sec, with three blades per rotor). The rotor blade radius is ~9 ft, and rotational speed is 577 RPM. The flight speed is 122 knots. The descent flight path angle is set at a 6° descent angle and the climb flight path is set at a 6° climb angle. For each of the turning flight cases, the turn rate 3°/sec, resulting in a vehicle bank (roll) angle of approximately 19°. Results are shown as Sound Exposure Level (SEL) ground noise maps for a square area of roughly 1,200 m x 1,200 m (3,940 ft x 3,940 ft). The number of ground observers is 6,561, in an 81x81 array. In level flight (straight and turning) the vehicle is flying 150 m (492 ft) above the ground. For climbing and descending flight (straight and turning), the flight path is constructed such that the vehicle is at 150 m altitude at [0 m, 0 m], the center of the ground area. In all cases the microphones are 1.22 m (4 ft) above the ground.

The CAMRAD II related predictions (trim and performance, vertical blade loading and its derivative) are the same as in Ref. 1. They are included in this paper for completeness. Some of the contour plots for loadz and its derivative in Ref. 1 needed improvement and updated versions are included. Additional discussion pertaining to the loadz derivative and how it relates to the loading noise is included.

The acoustics predictions presented here differ from those shown in Ref. 1. The current noise predictions incorporate changes associated with the acoustics tools, such as improvements and updates to the software codes and the run procedures. Also, to account for the upcoming updates to the Fly Neighborly recommendations, SEL ground noise contour

maps are shown instead of the OASPL and EPNL three ground microphone results that were shown in Ref. 1.

Results are presented separately for each maneuver condition and include the following:

- Trim and performance quantities.
- Contour plots (front right rotor, # 1) for the vertical blade loading ("loadz") and its derivative. loadz is in the airframe frame, with negative loadz (-loadz) positive up.
- Azimuthal loadz and its derivative at a reprentative outboard blade spanwise location (0.765R).
- SEL ground noise maps.

Level turns

Quadrotor trim and performance, level turns. Results for level straight flight and level turns are shown in Figs. 3a-3i. The trim and performance quantities shown include the blade collective, vehicle pitch and roll, rotor thrust and power. Figures 3a-3b show the average collective and vehicle pitch and roll angles required for trim. Figure 3f shows that the interference power is very small (with small increases in the rear rotors, # 3 and 4); Fig. 3e shows the same effect for the total power. Propulsive power (Fig. 3i) is the largest contributor to the total power. The induced and profile powers are roughly of the same magnitude (Figs. 3g-3h) and contribute equally to the total power.

Derivative of vertical blade loading, level turns. Results for only the front right rotor (# 1) are shown here because, for the 122 knots flyover considered in this study, rotor-rotor interference is small (Fig. 3f) compared to the 50 knots approach condition considered in Refs. 4 and 6 where the rear rotors are significantly influenced by the front rotors. Also, the front two rotors behave similarly, and basic trends can be obtained from a study of only the front right rotor. Figures 4a-4d show vertical blade loading contours and azimuthal variations at the 0.765R radial station (represented by the dashed-line circle in Figs. 4a-4c) for level flight and level turns. Figures 5a-5d show the corresponding loadz derivatives.

The vertical blade loading derivative loadz is important because it is a leading contributor to the far field loading noise. This can be seen from the full surface acoustics equation below (Ref. 16). Even though the compact line model is used in the present computational model, basic effects may be identifiable. The loading noise component, p'_L, of Farassat's Formulation 1A (F1A, see Ref. 13 also) is:

$$4\pi p'_L(\mathbf{x},t) = \int_{f=0}\left[\frac{\dot{p}\cos\theta}{c\,r\,(1-M_r)^2} + \frac{\hat{r}_i\dot{M}_i\,p\cos\theta}{c\,r\,(1-M_r)^3}\right]_{\text{ret}} dS + \quad \text{Far field}$$

$$\int_{f=0}\left[\frac{p(\cos\theta - M_i\,n_i)}{r^2\,(1-M_r)^2} + \frac{(M_r - M^2)\,p\cos\theta}{r^2\,(1-M_r)^3}\right]_{\text{ret}} dS \quad \text{Near field}$$

Broadly, the derivative of the loading p (the p dot term) is the largest contributes to the far field loading noise (the $1/r$ term, where r is the distance from the source to the observer). The precise meanings of all the quantities in the equation can be found in Ref. 16. As shown later under noise results, thickness noise is not an important contributor to the total noise for the flight conditions considered in this study and is not discussed in this study.

The increased loading during turns is shown in Figs. 4a-4d, see the region near the front of the rotor (red-orange color region). The contours for the left and right turns are largely similar (Figs.4b-4c), with slight variations between them (this can also be seen from Fig. 4d). Figures 4a-4d show "hot spots" are around 0° and 180° azimuths, i.e., the typical 2 per rev behavior in forward flight, seen clearly in Fig. 4d. Some BVI activity is seen in the 45°-90° range which can be identified via loading spikes. Figures 5a to 5c show slightly increased BVI occurrences during turns compared to level flight. The spikes in the azimuthal derivatives of loadz shown in Fig. 5d are consistent with the above observations, showing corresponding spikes. Figure 5d is similar in shape to a typical BVI time history that is seen in rotorcraft noise literature (for example, Fig. 6 of Ref. 17).

Quadrotor noise, level turns. For straight level flight, Figs. 6a-6c show the broadband self noise, loading noise and total noise, respectively. The thickness noise underneath the vehicle is small (~60 dBA) compared to the loading noise, so it is not shown here. Figures 6a-6c show that the total noise is primarily loading noise. Figures 7a-7c show the corresponding results for a level left turn – the loading noise is the primary contributor to total noise. However, for this curved flight path (the left turn) noise increases in the direction opposite to the turn – noise is higher on the right side (Fig. 7c). Since the total noise is mostly loading noise and with the vehicle tilted (banked) to the left, the noise should move to the right because the right side of the flight path is now "below" the vehicle. Figure 8 shows the total noise for a level right turn; the conclusions are the same as for the left turn.

Fly Neighborly considerations, level turns. The relevant current recommendations are in italics.

a) *Straight flight is quieter than turning flight*. Figures 6c, 7c, and 8 show that this recommendation is not followed by this quadrotor under the flight conditions examined – here, turning flight is quieter than straight flight. May be related to the effect of multiple rotors. Needs further study.

b) *Turning away from the advancing blade ... is quieter than turning into the advancing blade*. This recommendation is not relevant for symmetric aircraft such as a quadrotor.

c) Importantly, noise increases in a direction opposite to the turn for this particular quadrotor under these flight conditions (Figs. 7c and 8). This finding may need to be taken into

consideration in formulating the upcoming updated Fly Neighborly recommendations.

Descending turns

Quadrotor trim and performance, descending turns. Results for descending turns are shown in Figs. 9a-9i. Figures 9a-9b show the average collective and vehicle pitch and roll angles required for trim. Figure 9f shows that the interference power is small relative to the total power (Fig. 9e), with increased power required for the rear rotors, # 3 and 4. The induced and profile powers are roughly of the same magnitude (Figs. 9g-9h) and contribute equally to the total power.

Derivative of vertical blade loading, descending turns. Results for only the front right rotor (# 1) are shown, as discussed in the section on level turns. Figures 10a-10d show vertical blade loading loadz contours and azimuthal variations at the 0.765R radial station for straight line descent and descending turns. Figures 11a-11d show the corresponding loadz derivatives. The increased loading during turns can be seen in Figs. 10a-10d. The contours for the left and right turns are largely similar (Figs.10b-10c), with slight variations between them (this can also be seen from Fig. 10d). Figures 10a-10d also show considerable BVI activity in descent and descending turns; several hot spots are present between 0° and 180° azimuths. At 0.765R, there is considerable BVI activity in the 0°-135° range which shows loading spikes (Fig. 10d). Figures 11a-11d show the corresponding derivatives.

Quadrotor noise, descending turns. Figures 12a-12c show the total noise predictions for straight line descent and left and right descending turns, respectively. All flight paths maintain the vehicle 150 m above ground at the center of the prediction square. Descending flights have higher noise levels compared to level maneuvers (compare Figs. 6c, 7c, 8 with Figs. 12a-12c).

Fly Neighborly considerations, descending turns. The relevant recommendations are in italics.

a) *Level turns are quieter than descending turns*. This recommendation is followed by this quadrotor under the flight conditions examined – here, descending flight involves higher noise levels compared to level flight (compare Figs. 6c, 7c, and 8 with Figs. 12a-12c). Descent generally involves increased BVI activity, and this conclusion may be reflecting this basic physical phenomenon common to all rotorcraft (with single or multiple main rotors).
b) *Straight-in [descending] flight is quieter than turning flight.* This recommendation is not followed by this quadrotor under the flight conditions examined – here, the maximum noise level is higher in straight flight compared to the maximum noise in descending turns (compare Fig. 12a with Figs. 12b-12c). In these figures the noise scales are different to enable easier identification of the maximum SEL numerical values.

Climbing turns

Quadrotor trim and performance, climbing turns. Results for straight climb and climbing turns are shown in Figs. 13a-13i. Figure 13f shows that the interference power in climbing turns is very small, with the induced and profile powers roughly equal (Figs. 13g-13h). As expected, the propulsive and climb power (Fig. 13i) is the largest contributor to total power in this flight condition.

Derivative of vertical blade loading, climbing turns. Results for only the front right rotor (# 1) are shown, as has been discussed in previous sections. Figures 14a-14d show vertical blade loading loadz contours and azimuthal variations at the 0.765R radial station for straight climb and climbing turns. Figures 15a-15d show the corresponding loadz derivatives. The increased loading during turns can be seen in Figs. 14a-14d which show loadz. The contours for the left and right turns are largely similar (Figs.14b-14c), with slight variations between them (this can also be seen from Fig. 14d). Figures 14a-14d also show there is no BVI activity in climbing turns (due to the rotor wake being blown back). The only hot spots are around 0° and 180° azimuths, i.e., the typical 2 per rev behavior in forward flight, seen clearly in Fig. 14d.

Quadrotor noise, climbing turns. Figures 16a-16c show the predictions for straight line climb and left and right climbing turns, respectively. All flight paths maintain the vehicle 150 m above ground at the center of the prediction square. Compared to descending turns, climbing turns are quieter.

Fly Neighborly considerations, climbing turns. There are no guidelines addressing climbing flight at this time.

CONCLUSIONS

As a follow-on study to the 2024 paper by Kottapalli, Silva, and Boyd, this study further examined whether the VAI Fly Neighborly operational recommendations that are based on single main rotor/tail rotor configurations hold for an example of a UAM-class vehicle with multiple rotors. Compared to the 2024 study, improved acoustics tools were used. Predictions were made for three steady maneuvers: level turns, descending turns, and climbing turns (total of nine flight conditions). The 6-occupant quadrotor concept vehicle designed under the NASA Revolutionary Vertical Lift Technology (RVLT) Project was considered. The tip speed is 550 ft/sec, with three blades per rotor. The RVLT Toolchain was exercised using CAMRAD II, pyaaron/AARON/ANOPP2 and AMAT. AMAT provides functionality to acoustically model the curved flight paths associated with turning flight. Quadrotor vehicle trim and performance, contour plots of the vertical blade loading (loadz) and its derivative, and azimuthal variations at the 0.765R radial station of loadz and its derivative were studied. Quadrotor noise trends in maneuvers were analyzed using SEL ground noise maps.

Conclusions on the consistency of the Fly Neighborly operational recommendations for the UAM quadrotor under the flight conditions examined are as follows (the recommendations are in italics):

1. Level Flight: *Straight flight is quieter than turning flight*. The results show this recommendation results in greater noise for this quadrotor for the flight conditions examined – here, turning flight is quieter than straight flight. May be related to the effect of multiple rotors. Needs further study.
2. Turning Flight:
    a. *Turning away from the advancing blade … is quieter than turning into the advancing blade*. This recommendation is not relevant for symmetric aircraft such as a quadrotor.
    b. *Level turns are quieter than descending turns*. This recommendation is appropriate for this quadrotor for the flight conditions examined – here, descending flight involves higher noise levels compared to level flight. Descent generally involves increased BVI activity, and this conclusion may be reflecting this basic physical phenomenon common to all rotorcraft (with single or multiple main rotors).
    c. Importantly, unlike conventional helicopters with a single main rotor, quadrotor noise increased in a direction opposite to the turn. Since the total noise is mostly loading noise and with the vehicle tilted (banked), for example to the left, the noise should move to the right because the right side of the flight path is now "below" the vehicle. This conclusion may need to be taken into consideration in formulating the upcoming updated Fly Neighborly recommendations.
3. Descending Flight: *Straight-in flight is quieter than turning flight*. This recommendation results in greater noise for this quadrotor for the flight conditions examined – here, the maximum noise level was higher in straight flight compared to the maximum noise in descending turns. May be related to the effect of multiple rotors. Needs further study.
4. Climbing Flight: There are no guidelines that address climb.

Author contact:
Sesi Kottapalli sesi.b.kottapalli@nasa.gov
Doug Boyd d.d.boyd@nasa.gov

ACKNOWLEDGEMENTS

Insightful discussions with the following colleagues are gratefully acknowledged: Wayne Johnson, Gloria Yamauchi, Bill Warmbrodt, Chris Silva, and Leonard Lopes.

Support from the Revolutionary Vertical Lift Technology (RVLT) Project is gratefully acknowledged.

Resources supporting this work were provided by the NASA High-End Computing (HEC) Program through the NASA Advanced Supercomputing (NAS) Division at Ames Research Center.

REFERENCES

1. Kottapalli, S., Silva, C., and Boyd, D. D., Jr. "Applicability of Fly Neighborly Noise Recommendations to UAM Quadrotors Undergoing Steady Maneuvers," VFS 6th Decennial Aeromechanics Specialists' Conference, Santa Clara, CA, February 2024.
2. Vertical Aviation International (VAI)) Fly Neighborly guidelines: https://verticalavi.org/wp-content/uploads/2024/11/Fly-Neighborly-Tips-Flyer-2019.pdf
3. Silva, C. and Johnson, W., "Practical Conceptual Design of Quieter Urban VTOL Aircraft," VFS 77th Annual Forum Proceedings, Virtual, May 2021.
4. Kottapalli, S. and Silva, C., "Prediction of Quadrotor Acoustics Using RVLT Toolchain," VFS Aeromechanics for Advanced Vertical Flight Technical Meeting, San Jose, CA, January 2022.
5. Yamauchi, G., "A Summary of NASA Rotary Wing Research: Circa 2008–2018," NASA/TP 2019-220459, December 2019.
6. Kottapalli, S., Silva, C., and Boyd, D. D, Jr. "Effect of Rotor Blade Elasticity on UAM Quadrotor Acoustics," VFS 79th Annual Forum Proceedings, West Palm Beach, FL, May 2023.
7. Brentner, K. S. and Jones, H. E., "Noise Prediction for Maneuvering Rotorcraft," Paper AIAA 2000–2031, 6th AIAA/CEAS Aeroacoustics Conference Proceedings, Lahaina, HI, June 2000.
8. Brentner, K. S., Perez, G., and Brès, G. A., "Toward a Better Understanding of Maneuvering Rotorcraft Noise," Vertical Flight Society 58th Annual Forum Proceedings, Montreal, Canada, May 2002.
9. Greenwood, E., Schmitz, F. H, and Gopalan, G., "Helicopter External Noise Radiation in Turning Flight: Theory and Experiment," Vertical Flight Society 71st Annual Forum Proceedings, Virginia Beach, VA, May 2015.
10. Stephenson, J. H., Watts, M. E., Greenwood, E., and Pascioni, K. A., "Development and Validation of Generic Maneuvering Flight Noise Abatement Guidance for Helicopters," *Journal of the American Helicopter Society*, Vol. 67, 012012 (2022), DOI: 10.4050/JAHS.67.012012, 2022.

11. Johnson, W., "CAMRAD II, Comprehensive Analytical Model of Rotorcraft Aerodynamics and Dynamics," Johnson Aeronautics, Palo Alto, CA, 1992-1999.
12. Meyn, L., "Rotorcraft Optimization Tools: Incorporating Rotorcraft Design Codes into Multi-Disciplinary Design, Analysis, and Optimization," AHS Technical Meeting on Aeromechanics Design for Vertical Lift, San Francisco, CA, January 2018.
13. Lopes, L. V. and Burley, C. L, "ANOPP2 User's Manual," NASA/TM-2016-219342, October 2016.
14. Lopes, L. V., "ANOPP2 Mission Analysis Tool (AMAT)," UAM Noise Working Group (UNWG), Subgroup 1 Meeting, Hampton, VA, December 2022.
15. Rizzi, S. A., Letica, S. J., Boyd, D. D. Jr., and Lopes, L. V., "Prediction of Noise-Power-Distance Data for Urban Air Mobility Vehicles," *Journal of Aircraft*, https://doi.org/10.2514/1.C037435, October 2023.
16. Farassat, F., "Derivation of Formulations 1 and 1A of Farassat," NASA/TM-2007-214853, March 2007.
17. Yamauchi, G. K., Signor, D. B., Watts, M. E., Hernandez, F. J., and LeMasurier, P., "Flight Measurement of Blade-Vortex-Interaction Noise Including Comparison with Full-Scale Wind Tunnel Data," American Helicopter Society 49th Annual Forum Proceedings, St. Louis. MO, May 1993. Also published as NASA-TM-112385, 1993.

1a). Six-occupant quadrotor isometric view, marked with rotor rotation direction and numbering.

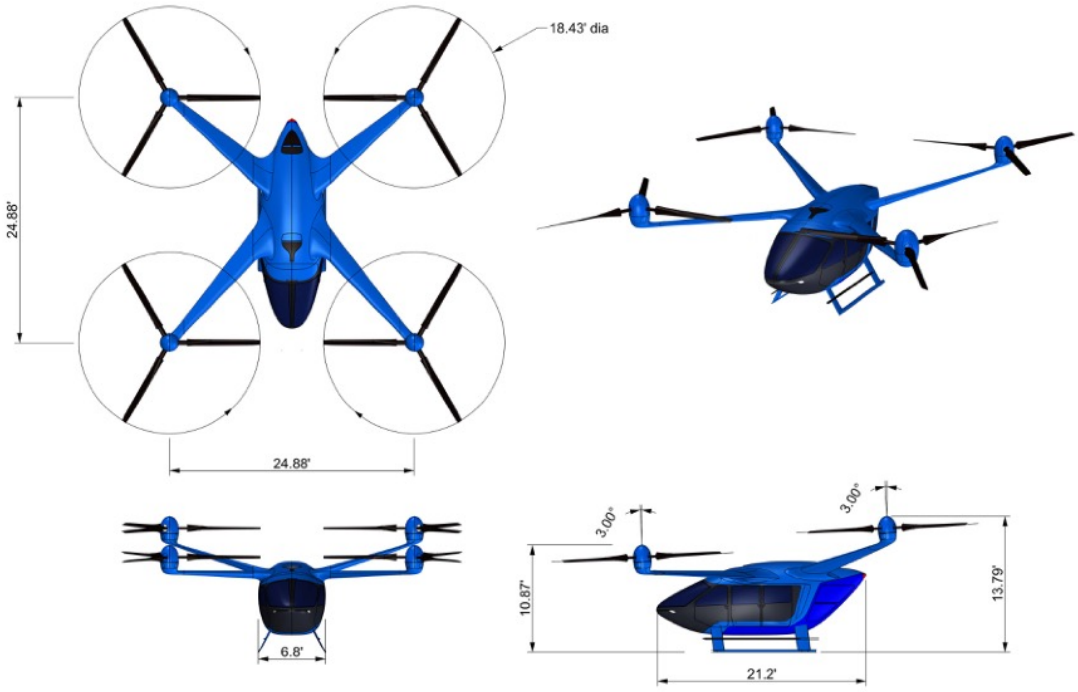

1b). Quadrotor three-view and oblique view.

Figure 1. Quadrotor geometry (Ref. 3).

Summary of Simulation Conditions

Flight speed is 122 knots

Straight and turning flight: level, climbing, and descending

(total of 9 flight conditions)

- Turns at 3 deg/sec
  (19 deg bank, 1.05 g's)
- Descent / climb at 6 deg
  (1,291 ft/min)

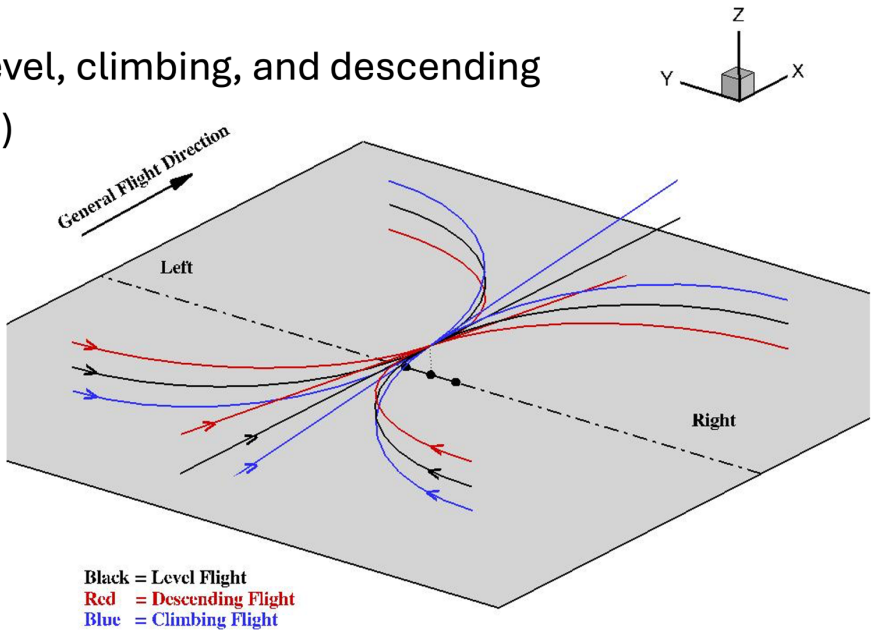

Figure 2. Summary of flight conditions and semi-circular (steady state) flight paths used in acoustic modeling of level, descending, and climbing turns. Curved lines depict flight paths for turns in both directions. Each path starts closest to the reader and ends away from the reader.

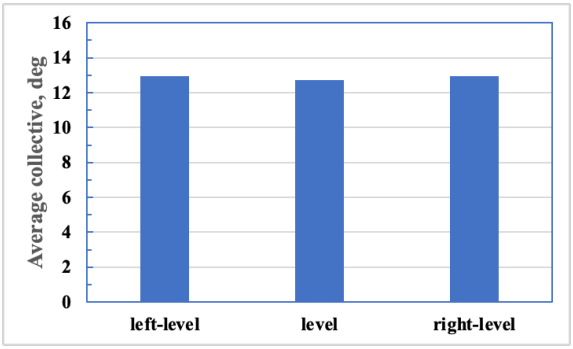

Figure 3a. Collective, average, level flight and level turns.

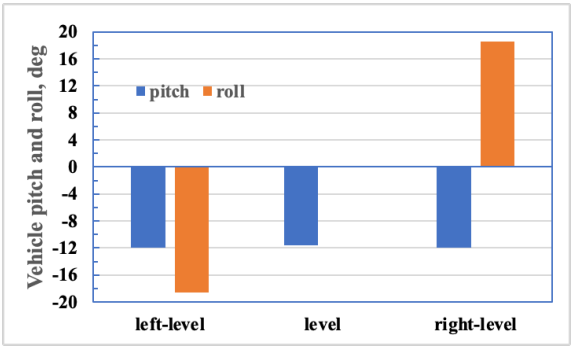

Figure 3b. Vehicle pitch and roll, level flight and level turns.

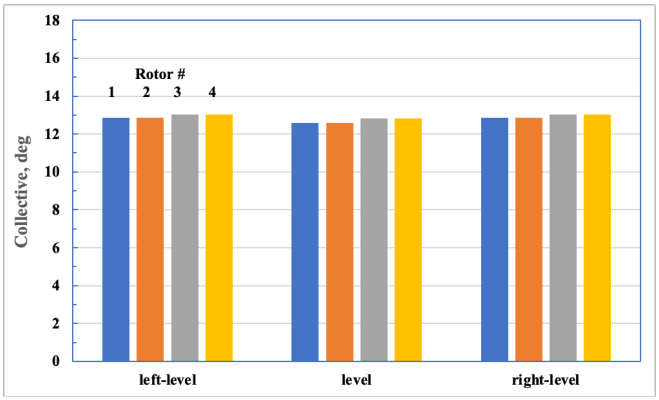

Figure 3c. Collective, rotors 1-4, level flight and level turns.

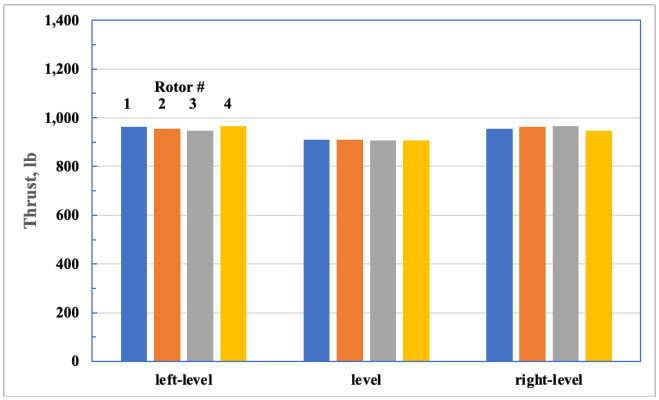

Figure 3d. Thrust, rotors 1-4, level flight and level turns.

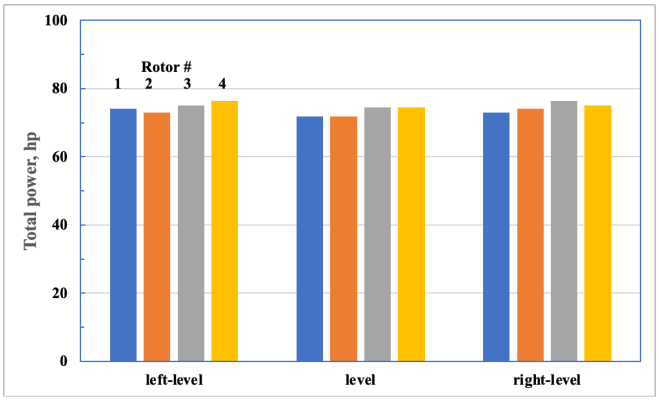

Figure 3e. Total power, level flight and level turns.

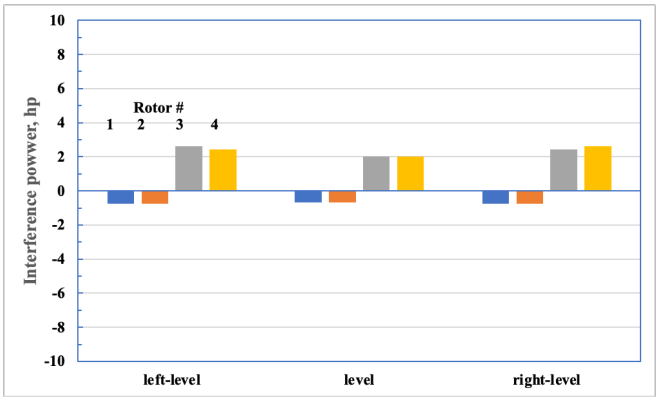

Figure 3f. Interference power, level flight and level turns.

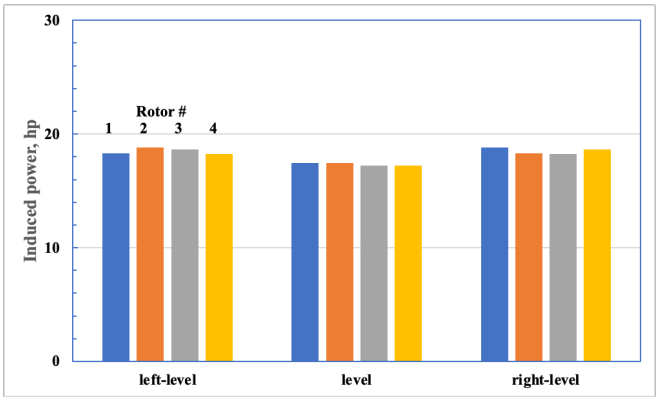

Figure 3g. Induced power, level flight and level turns.

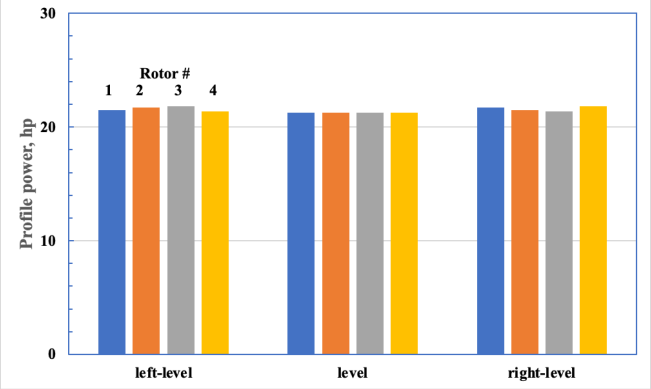

Figure 3h. Profile power, level flight and level turns.

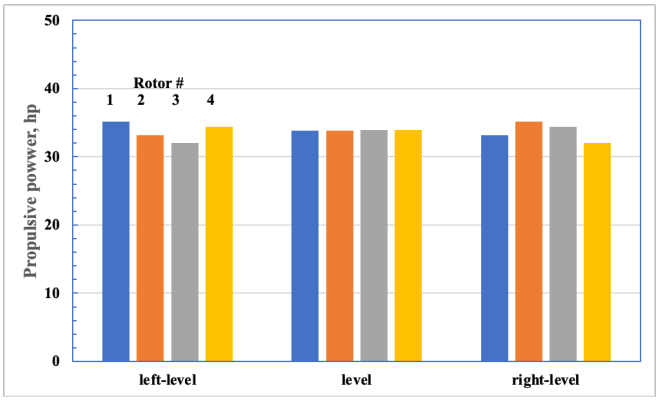

Figure 3i. Propulsive power, level flight and level turns.

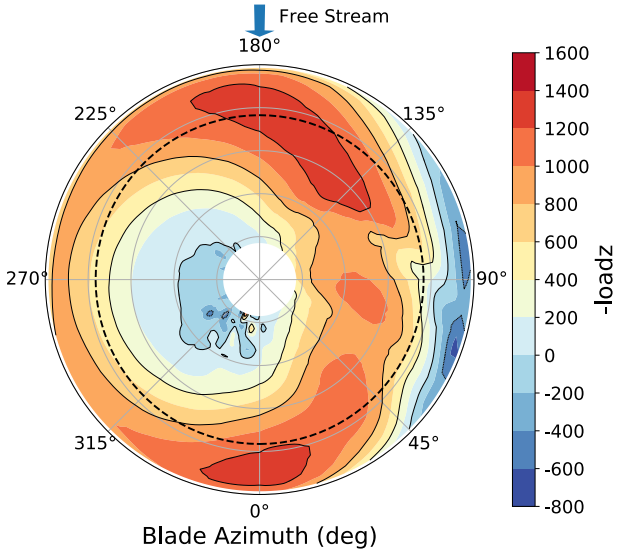

Figure 4a. loadz, level flight.

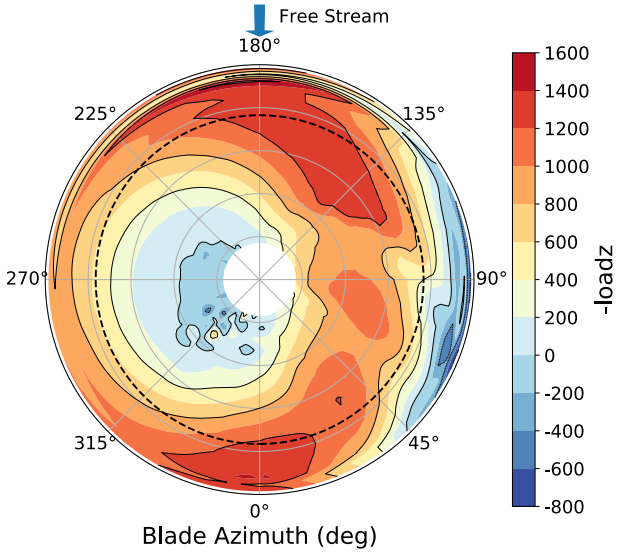

Figure 4b. loadz, level left turn.

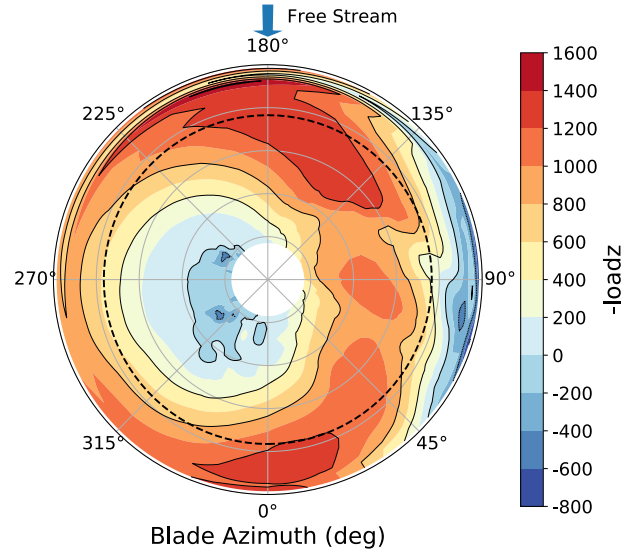

Figure 4c. loadz, level right turn.

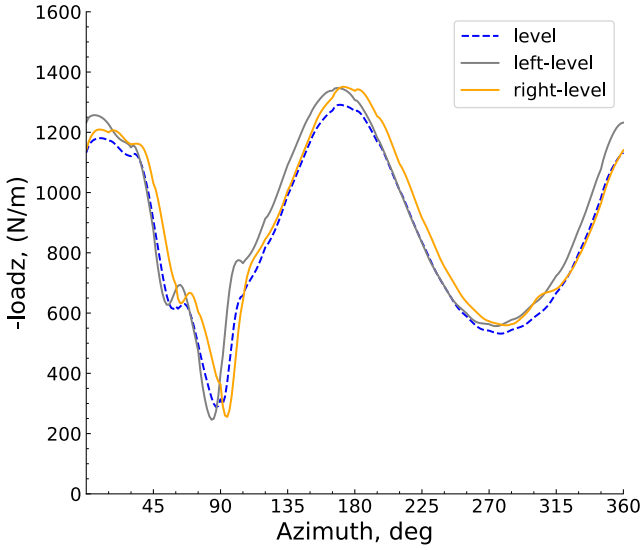

Figure 4d. 0.765R (dashed-line circle, Figs. 4a-4c) loadz, level turns.

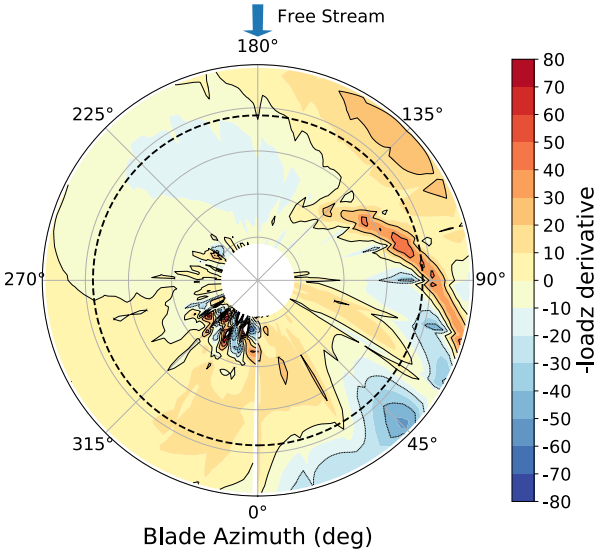

Figure 5a. loadz derivative, level flight.

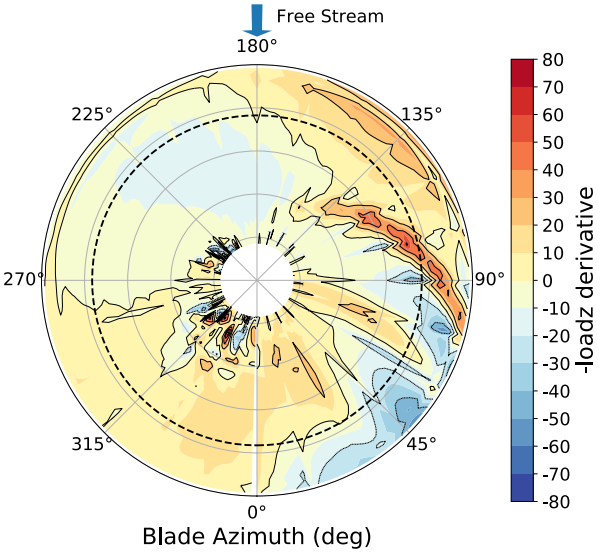

Figure 5c. loadz derivative, level right turn.

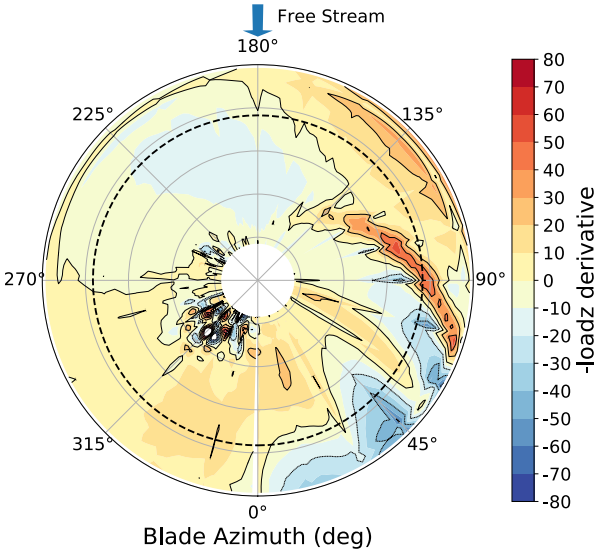

Figure 5b. loadz derivative, level left turn.

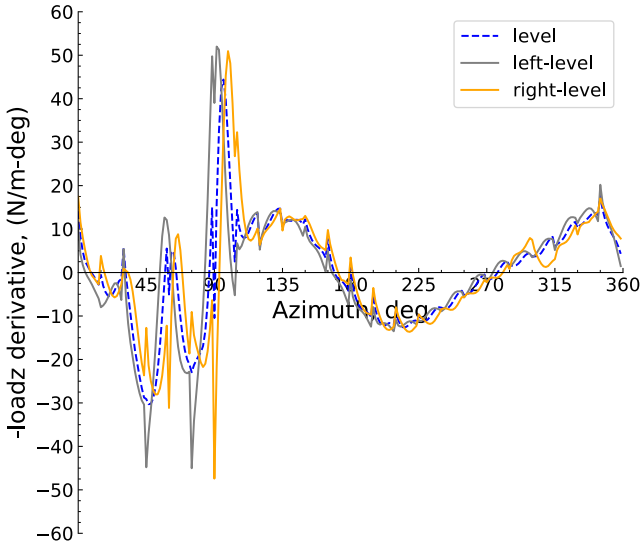

Figure 5d. 0.765R (dashed-line circle, Figs. 5a-5c) loadz derivative, level flight and level turns.

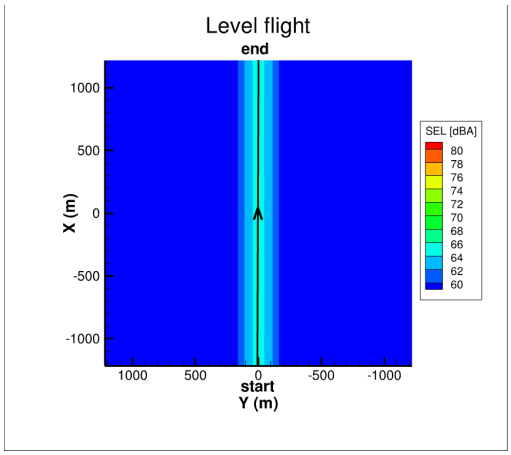

Figure 6a. Broadband self-noise, level flight.

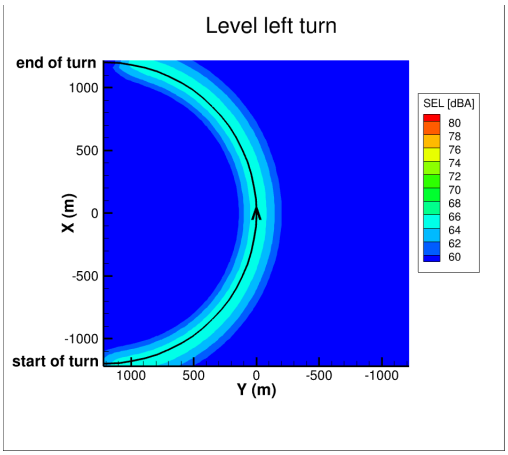

Figure 7a. Broadband self-noise, level left turn.

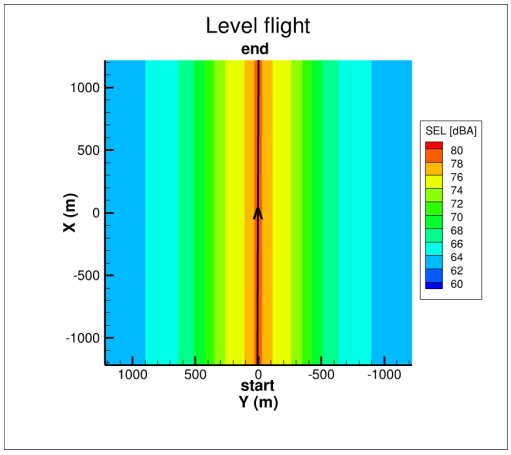

Figure 6b. Loading noise, level flight.

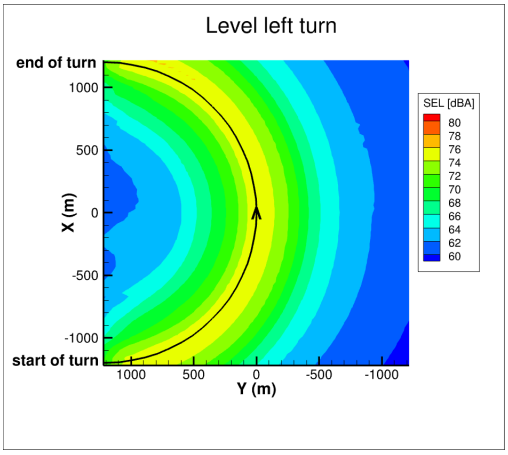

Figure 7b. Loading noise, level left turn.

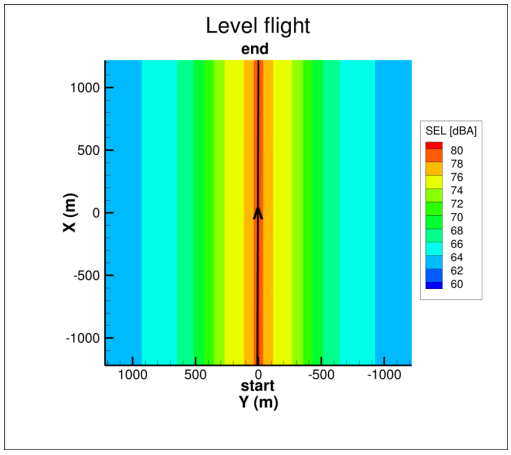

Figure 6c. Total noise, level flight.

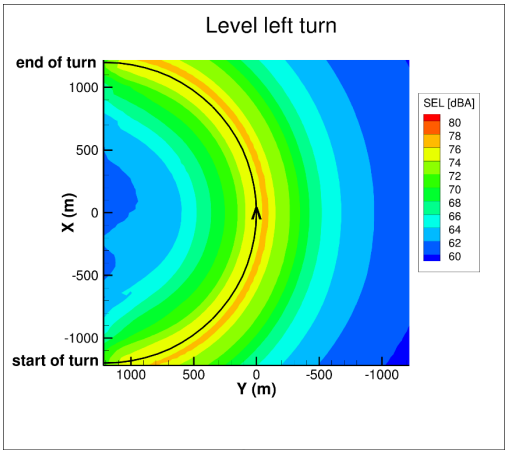

Figure 7c. Total noise, level left turn.

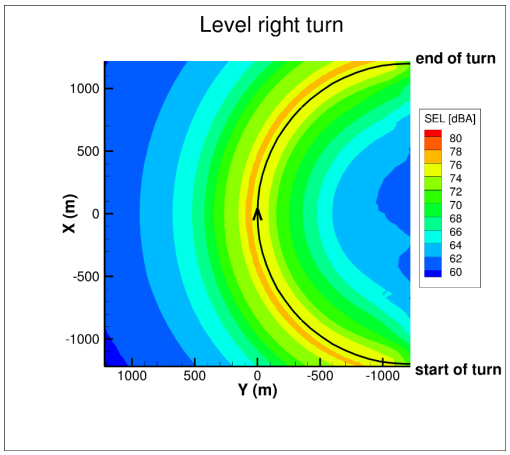

Figure 8. Total noise, level right turn.

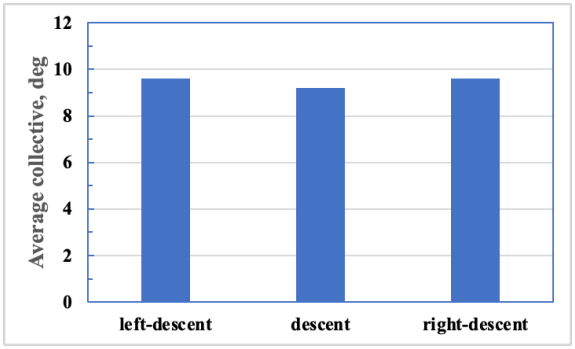

Figure 9a. Collective, average, descending flight and descending turns.

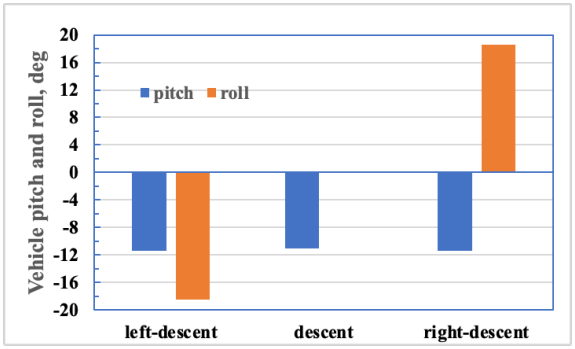

Figure 9b. Quadrotor pitch and roll, descending flight and descending turns.

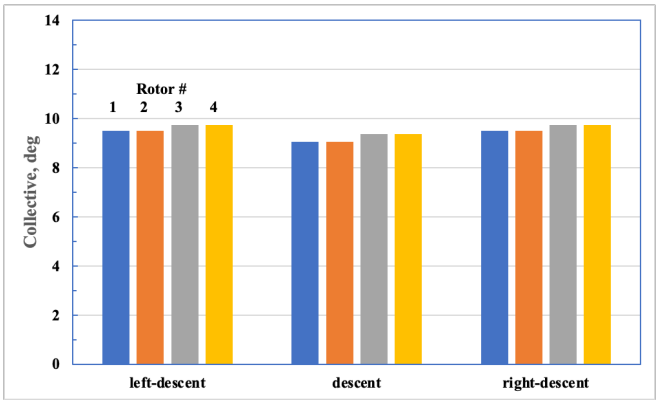

Figure 9c. Collective, rotors 1-4, descending flight and descending turns.

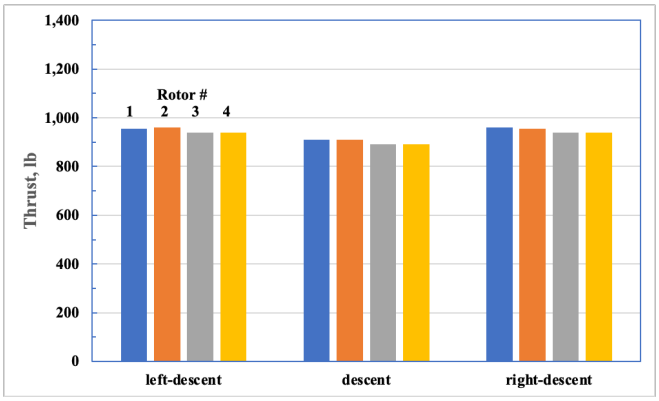

Figure 9d. Thrust, rotors 1-4, descending flight and descending turns.

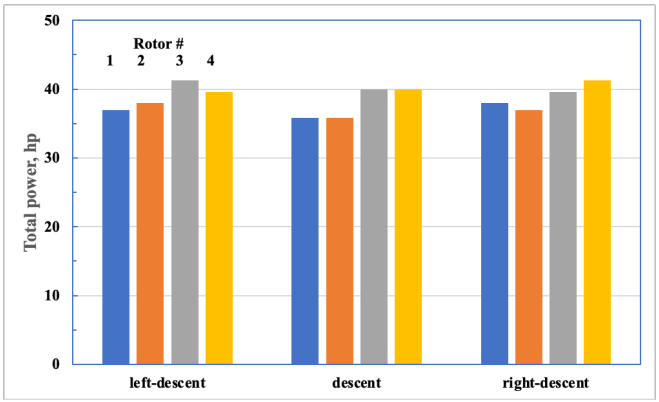

Figure 9e. Total power, descending flight and descending turns.

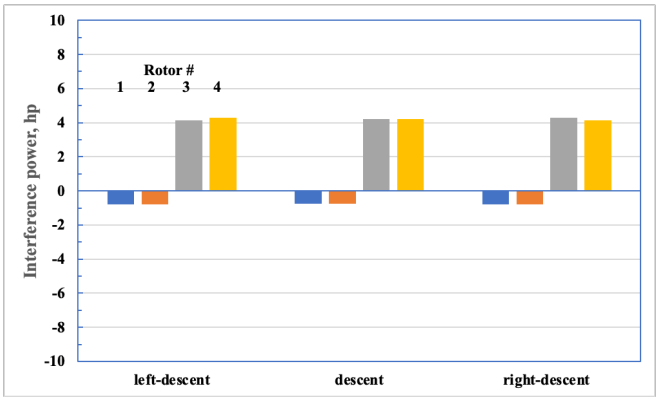

Figure 9f. Interference power, descending flight and descending turns.

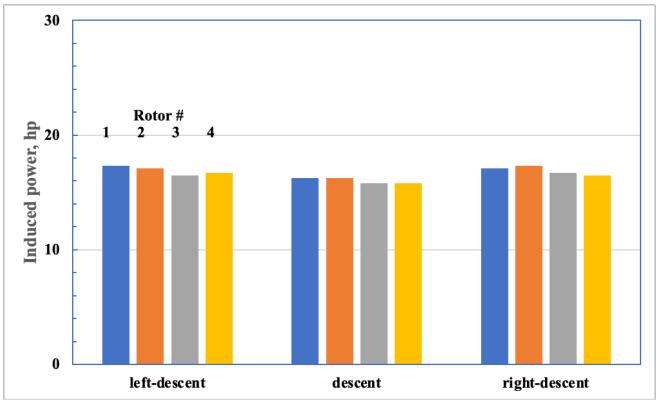

Figure 9g. Induced power, descending flight and descending turns.

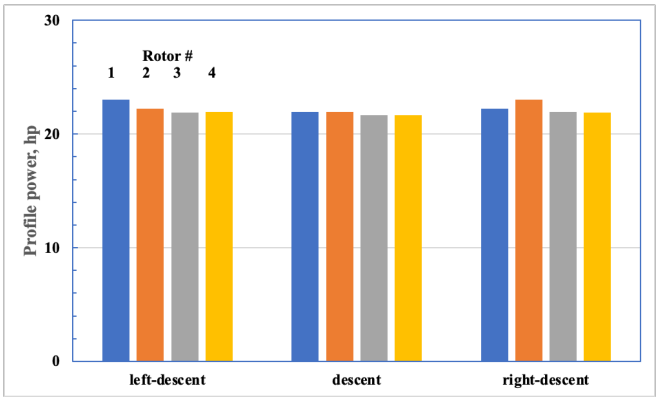

Figure 9h. Profile power, descending flight and descending turns.

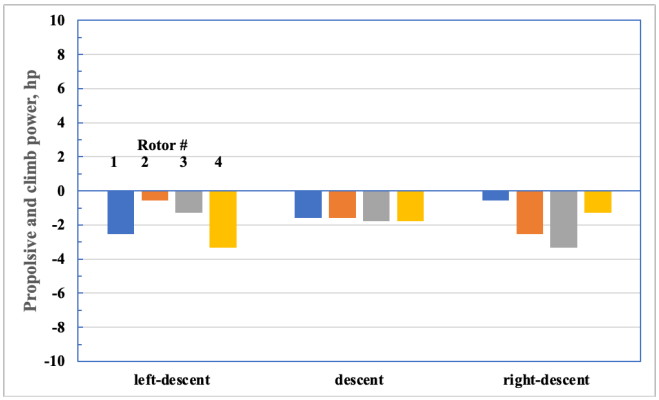

Figure 9i. Propulsive and climb power, descending flight and descending turns.

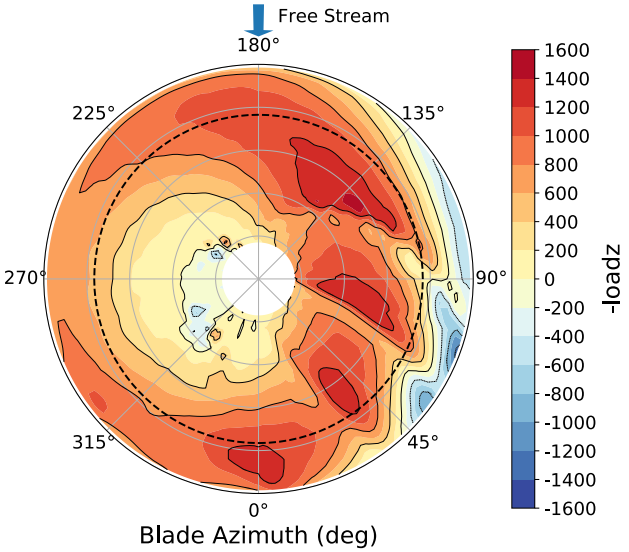

Figure 10a. loadz, descent.

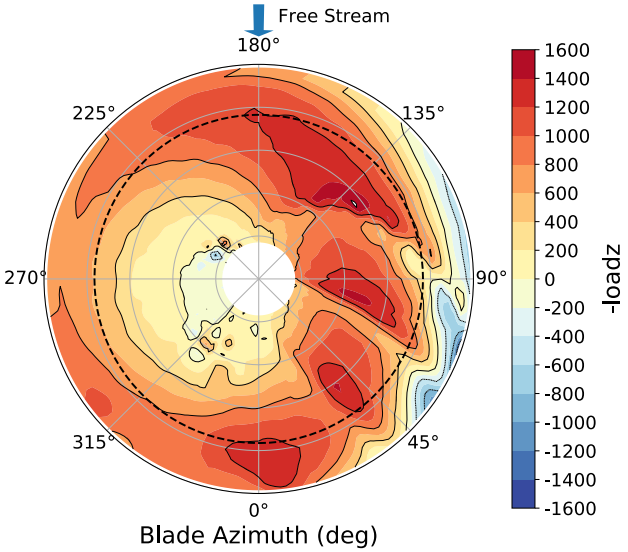

Figure 10c. loadz, descending right turn.

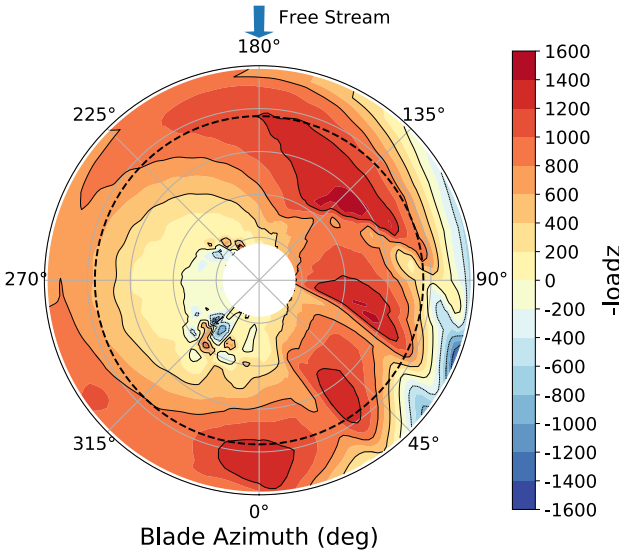

Figure 10b. loadz, descending left turn.

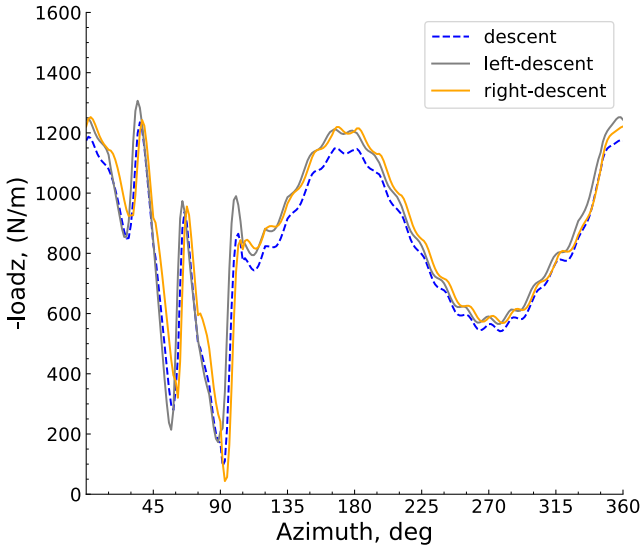

Figure 10d. 0.765R (dashed-line circle, Figs. 10a-10c) loadz, descending flight and descending turns.

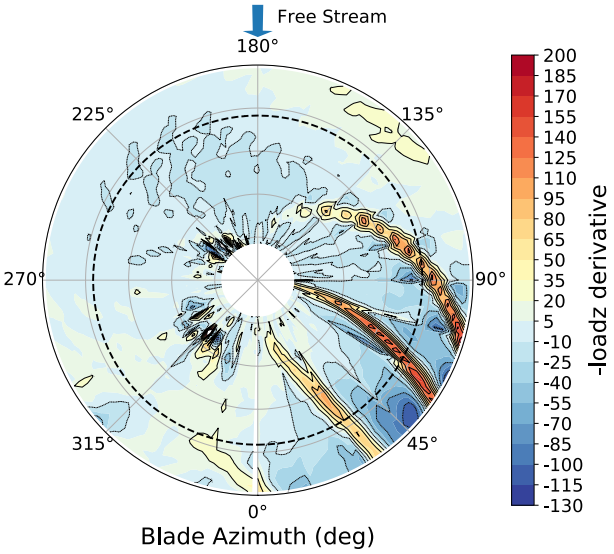

Figure 11a. loadz derivative, descent.

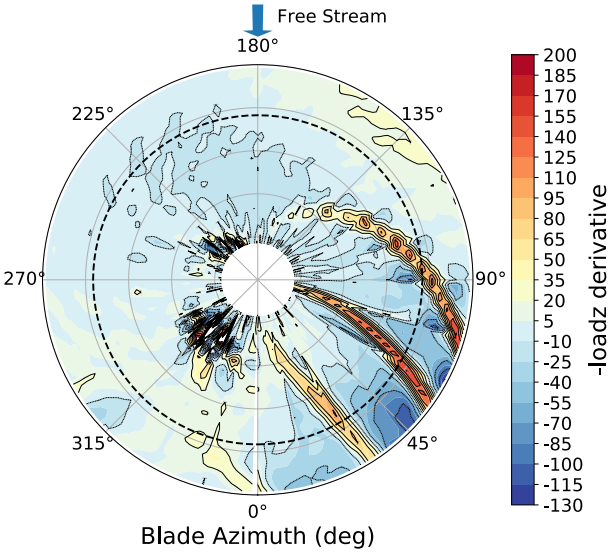

Figure11b. loadz derivative, descending left turn.

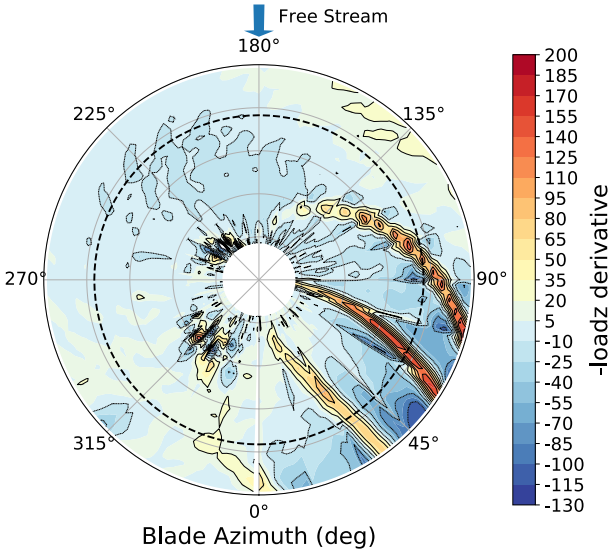

Figure 11c. loadz derivative, descending right turn.

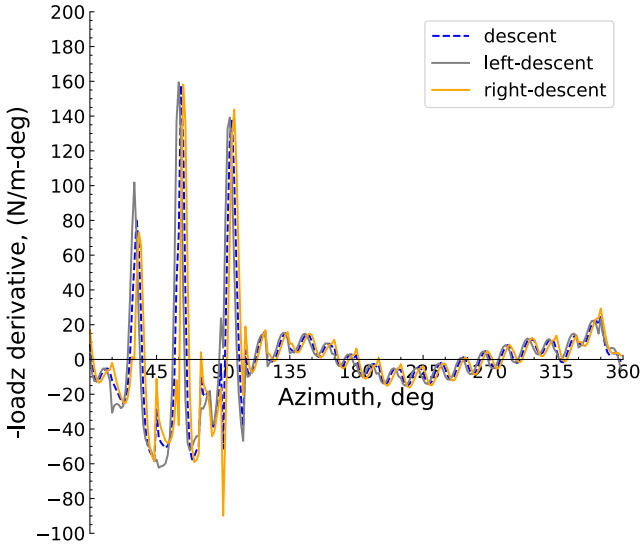

Figure 11d. 0.765R (dashed-line circle, Figs. 11a-11c) loadz derivative, descending flight and descending turns.

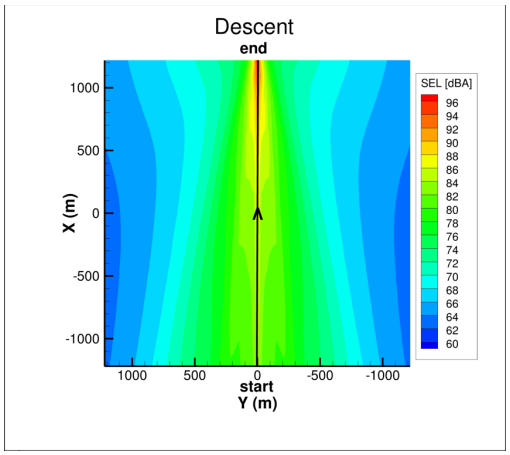

Figure 12a. Total noise, descent.

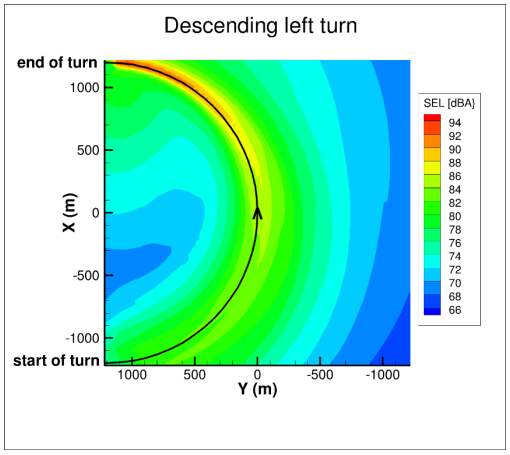

Figure 12b. Total noise, descending left turn.

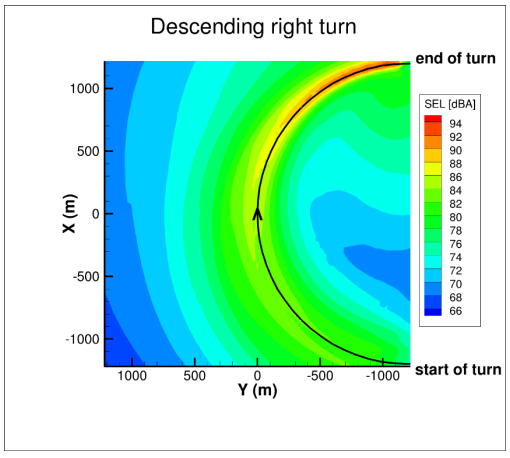

Figure 12c. Total noise, descending right turn.

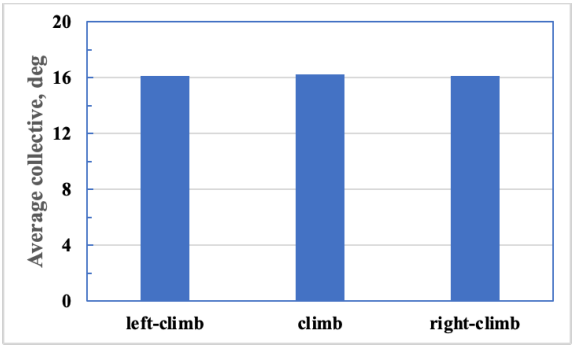

Figure 13a. Collective, average, climb and climbing turns.

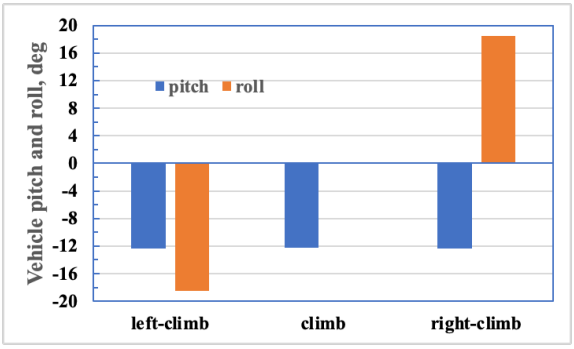

Figure 13b. Quadrotor pitch and roll, climb and climbing turns.

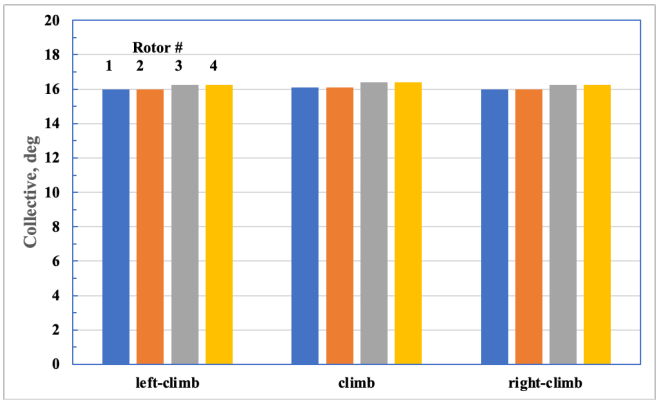

Figure 13c. Collective, rotors 1-4, climb and climbing turns.

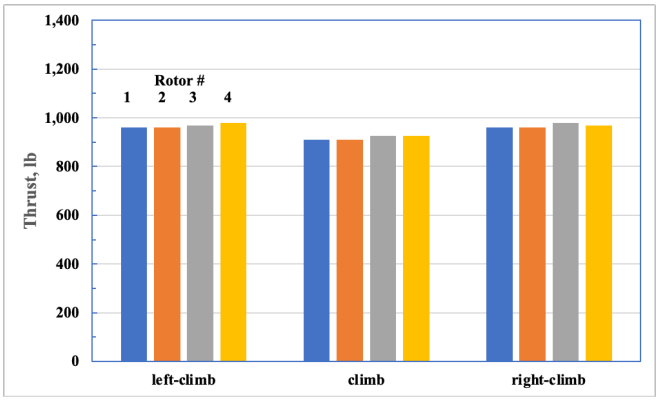

Figure 13d. Thrust, rotors 1-4, climb and climbing turns.

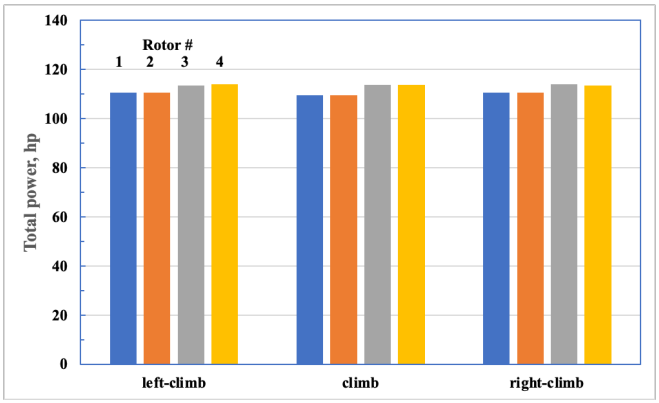

Figure 13e. Total power, climb and climbing turns.

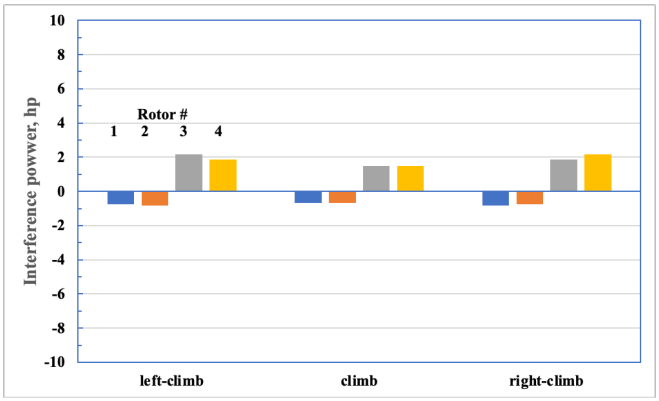

Figure 13f. Interference power, climb and climbing turns.

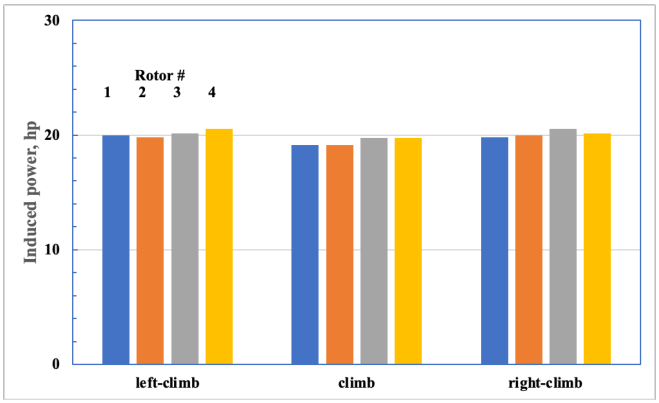

Figure 13g. Induced power, climb and climbing turns.

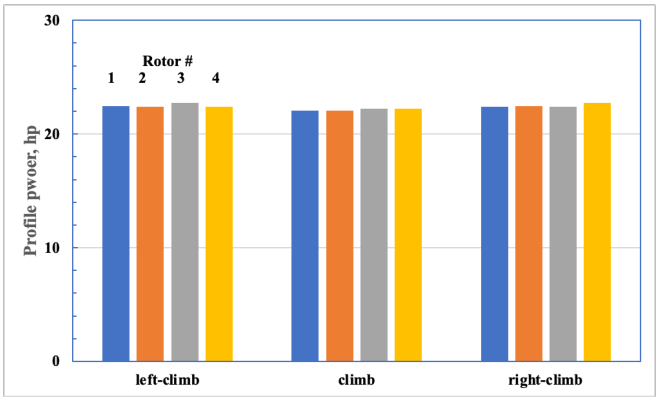

Figure 13h. Profile power, climb and climbing turns.

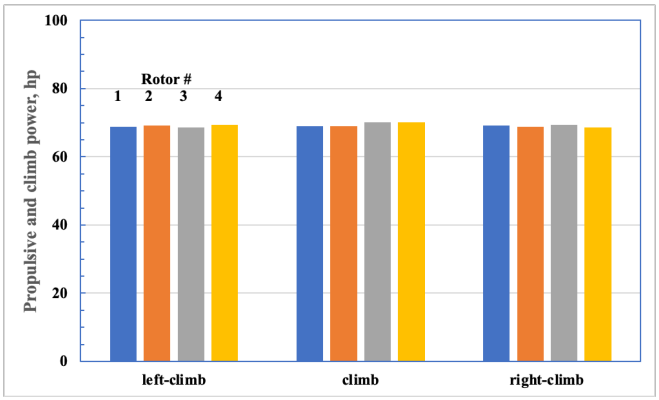

Figure 13i. Propulsive and climb power, climb and climbing turns.

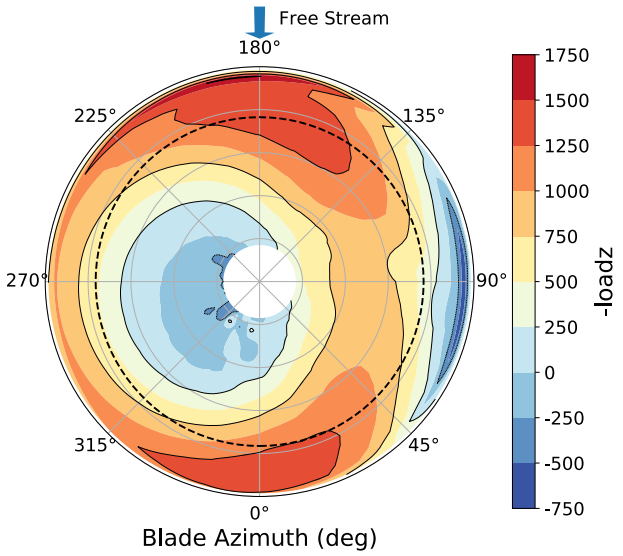

Figure 14a. loadz, climb.

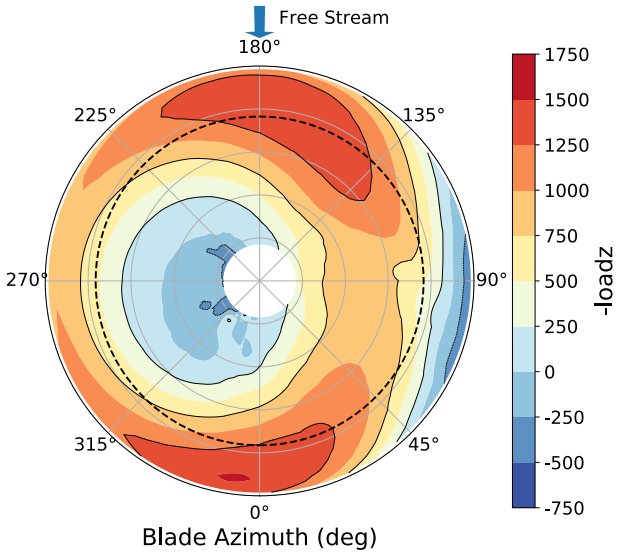

Figure 14b. loadz, climbing left turn.

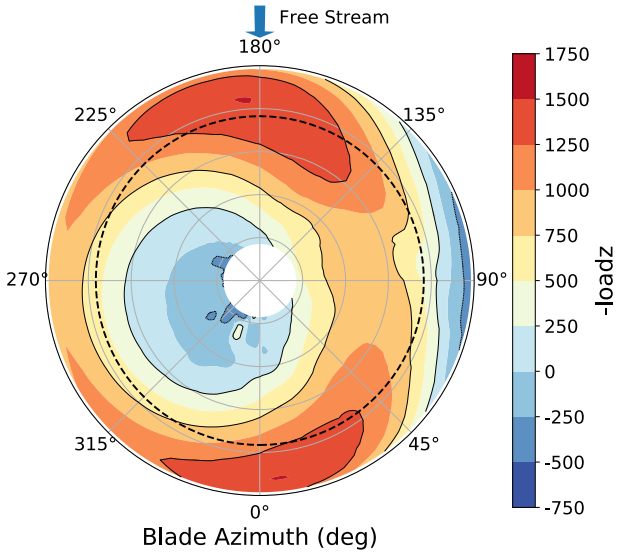

Figure 14c. loadz, climbing right turn.

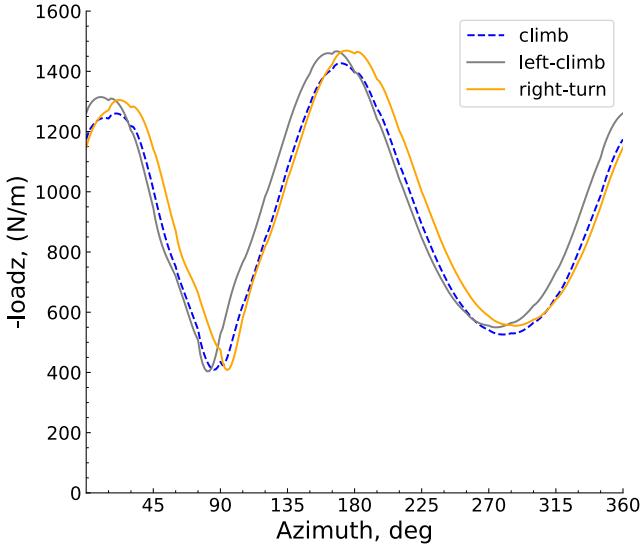

Figure 14d. 0.765R(dashed-line circle, Figs. 12a-12c) loadz, climbing turns.

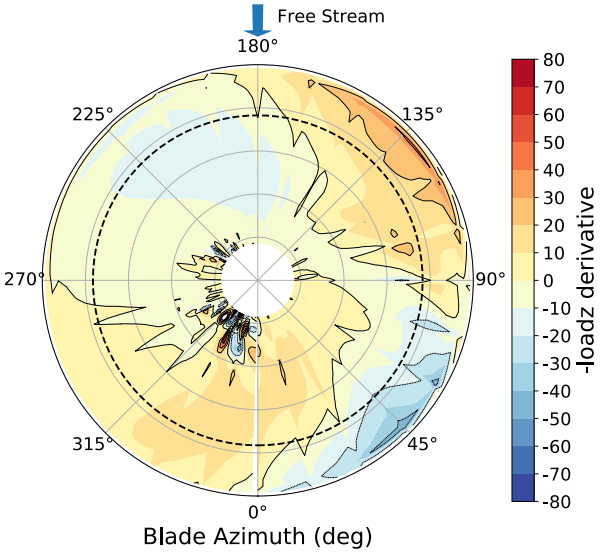

Figure 15a. loadz, derivative climb.

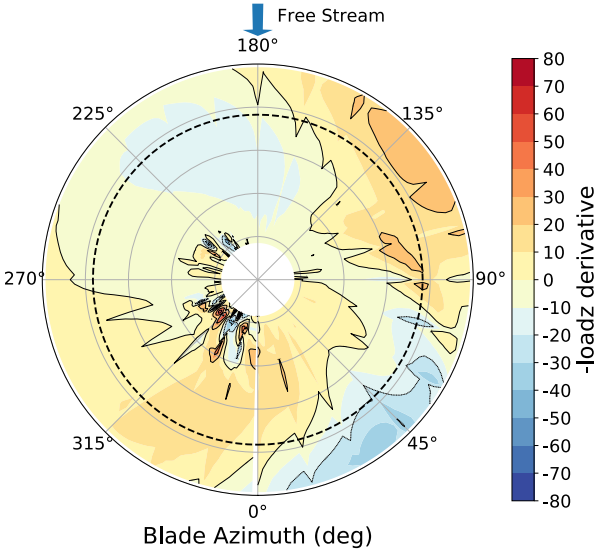

Figure 15b. loadz, derivative climbing left turn.

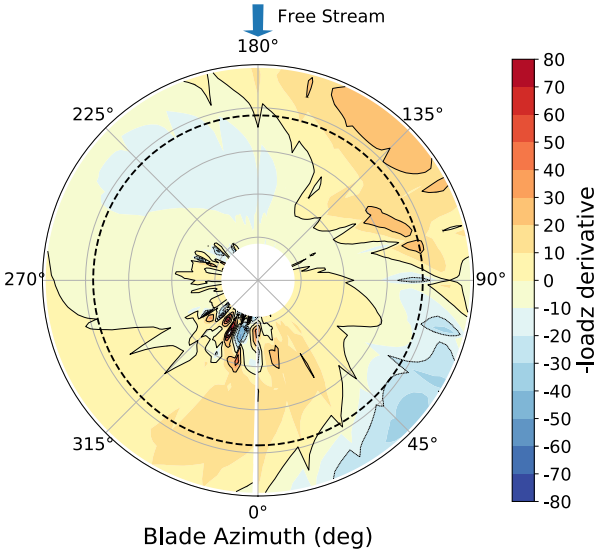

Figure 15c. loadz, derivative climbing right turn.

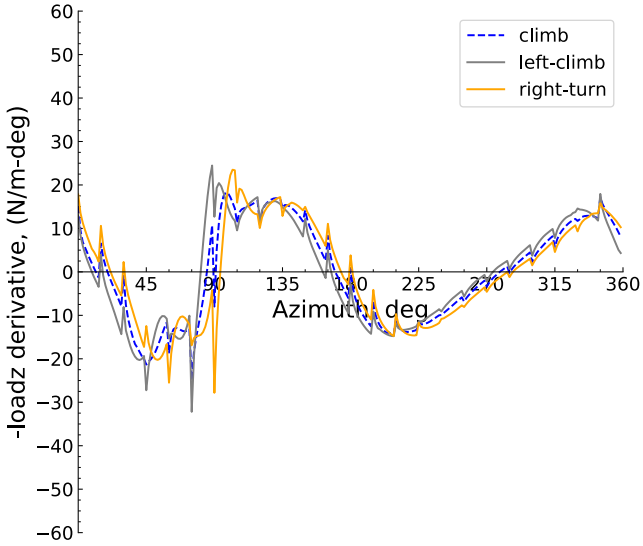

Figure 15d. 0.765R (dashed-line circle, Figs. 13a-13c) loadz derivative, climb and climbing turns.

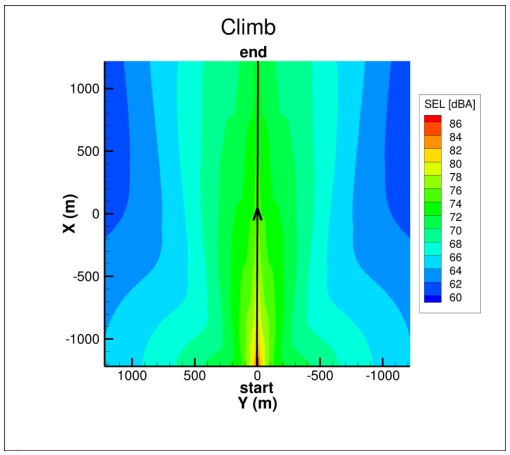

Figure 16a. Total noise, climb.

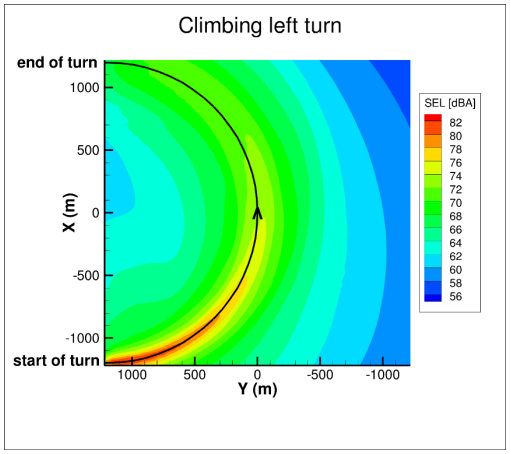

Figure 16b. Total noise, climbing left turn.

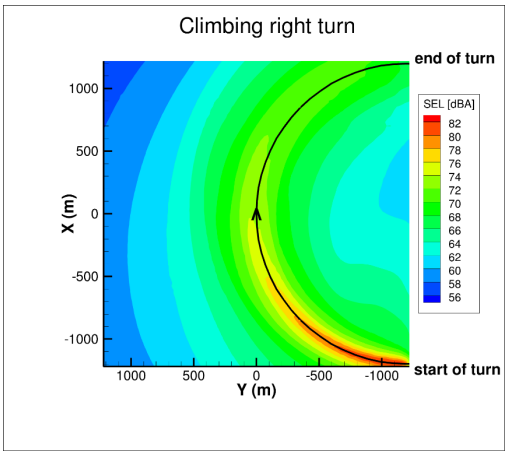

Figure 16c. Total noise, climbing right turn.